International Journal of Statistics and Applied Mathematics 2024; 9(1): 48-51

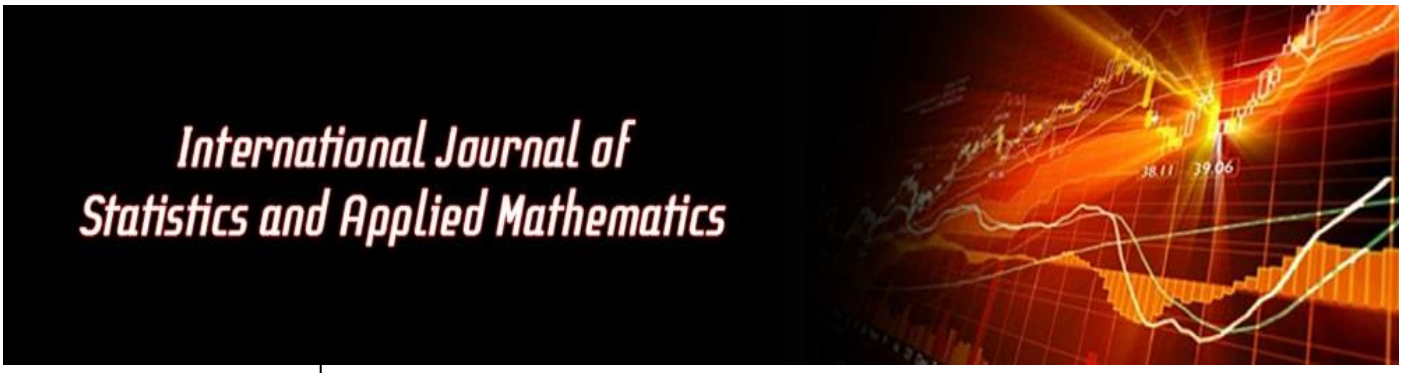

ISSN: 2456-1452
Maths 2024; 9(1): 48-51

https://www.mathsjournal.com
Received: 03-11-2023
Accepted: 02-12-2023

Chanda Thapliyal Nautiyal
Assistant Professor, (Mathematics), Department of Higher Education Uttarakhand, India

Corresponding Author:
Chanda Thapliyal Nautiyal
Assistant Professor, (Mathematics), Department of Higher Education Uttarakhand, India

Exploring protective window through the lens of image restoration techniques

Chanda Thapliyal Nautiyal

DOI: https://dx.doi.org/10.22271/maths.2024.v9.i1a.1599

Abstract
A comparative performance analysis of three distinct clutter reduction techniques, including Max, Harmonic, and Geometric filters, is done in this paper. This research proposes new algorithms for these three filters with protective windows to lessen the bias caused by the target. We compare these new methods with blurry images. It results in the crucial conclusion that the filter with the best performance in a certain circumstance should be chosen. The outcome of the experiment demonstrates that the suggested algorithms with the protective window are more effective than the current methods.

Keywords: SNR, max filter, harmonic-mean filter, geometric mean filter, protective window

Introduction
Image restoration techniques first appeared as a significant area of image processing during the Renaissance, when skilled restorers repaired damaged oil paintings by hand. However, there were several drawbacks to manual restoration, including the scarcity of specialists in the field and the time and danger involved. Image restoration techniques are extensively employed in diverse fields to salvage deteriorating film and eliminate extraneous information from images. Different methods used for restoration of deteriorated image involves partial differential equation-based strategies [1], Markov random field-based approaches [2], wavelet-based fusion techniques [3]. To restore the corrupted image to its original state, image restoration techniques are applied [4]. A number of restoration procedures exist, one of which is Blind Image DE convolution, which results in X-ray images that have a ringing appearance when restored [5]. Long-range correlation for image restoration was also suggested by some researchers [6].
Various direct and non-strategic separation techniques and de-noising computations have been developed to reduce the image noise. Straight channels tend to blur the boundaries of a picture; thus, they are not the best choice for effectively eliminating motivational commotion [7].
Wiener filter with optimal window technique was adopted to deal with the motion-blurred images and its performance in restoration of image was discussed. Li and Zhan compared several recovery algorithms and analyzed the reason for motion blur simulation images. Author studies image restoration methods based on Wiener filter and spatial difference technique, simulates the two methods, and analyses simulation results [8].

The present paper studies three smoothing techniques in this work. The following techniques are introduced along with a protective window
1. Max-Filter.
2. Harmonic Mean-Filter.
3. Geometric-Mean Divider.
4. Protective window-equipped with Max-Filter.
5. Protective window-equipped with Harmonic Mean-Filter.
6. Protective window-equipped with Geometric-Mean-Filter.

Problem description: The mathematical equation is expressed as follows using the model in [9] rebuild the starting image u* from noisy and blurry observation t*.

The mathematical equation is expressed as follows using the model in [9] rebuild the starting image u* from noisy and blurry observation t*.

$$t^*(i,j) = u^*(i,j)\ c^*(i,j) + o^*(i,j)$$

In this case, u* c* represents the convolution of the initial image u* with a blur operator c*, and o* represents noise. The average filter is used as a blur operator (c*) in this study.
The noise removal process involves subtracting the estimated background *b(i, j)* obtained by filtering from the original image 't'. After clutter is removed, the generic pixel is $z(i,j) = t^*(i,j) - b(i,j)$

The following filters are used to determine *b (i, j)* in this paper

A. Max Filter: A crucial component of low-level vision and image processing is the max filter. It is the same as the morphological operation in mathematics, dilation. This filter finds the grey level values of the brightest pixels.
In mathematical terms, the background estimations *b(i,j)* by the Max-filter can be represented as

b_{Max} max {a1, a2, a3, a4}
Where

$$a_1 = \{t(i, j-N), \dots, t(i,j), \dots, t(i, j+N)\}$$
$$a_2 = \{t(i-N, j), \dots, t(i,j), \dots, t(i+N, j)\}$$
$$a_3 = \{t(i+N, j-N), \dots, t(i,j), \dots, t(i-N, j+N)\}$$
$$a_4 = \{t(i-N, j-N), \dots, t(i,j), \dots, t(i+N, j+N)\}$$

It lessens the difference in intensity between neighbouring pixels. This technique for image smoothing is simple to use and lessens the fluctuation in intensity between consecutive pixels. The maximum selection processing in the sub image region is the outcome of this filter.

B. Harmonic Mean-Filter: The harmonic mean of the values of the pixels in a surrounding area is used to replace each pixel's value in the harmonic mean filter approach.

This filter yields the following background estimates *b(i, j)*

b_{hmean} max {a1,a2, a3, a4}
Where

$$a_1 = \text{harmonicmean}\{t(i, j-N), \dots, t(i,j), \dots, t(i, j+N)\}$$
$$a_2 = \text{harmonicmean}\{t(i-N, j), \dots, t(i,j), \dots, t(i+N, j)\}$$
$$a_3 = \text{harmonicmean}\{t(i+N, j-N), \dots, t(i,j), \dots, t(i-N, j+N)\}$$
$$a_4 = \text{harmonicmean}\{t(i-N, j-N), \dots, t(i,j), \dots, t(i+N, j+N)\}$$

C. Geometric Mean-Filter: By considering the surrounding features and reducing the variation, the geometric mean filter replaces the grey level of a pixel. This attenuates noise. The median and geometric mean filters exceed the arithmetic mean filter in decreasing noise while keeping edge details; this filter is called a smoothing spatial filter. A member of the nonlinear mean filter set is the geometric mean filter. The geometric mean filter's background estimations *b(i,j)* can be written as follows:

$b_{geomean}$ = max {a1, a2, a3, a4}
Where

$$a_1 = \text{geomean}\{t(i, j-N), \dots, t(i,j), \dots, t(i, j+N)\}$$
$$a_2 = \text{geomean}\{t(i-N, j), \dots, t(i,j), \dots, t(i+N, j)\}$$
$$a_3 = \text{geomean}\{t(i+N, j-N), \dots, t(i,j), \dots, t(i-N, j+N)\}$$
$$a_4 = \text{geomean}\{t(i-N, j-N), \dots, t(i,j), \dots, t(i+N, j+N)\}$$

Proposed protective window for the max, harmonic, and Geomean Filter

The directional operations become biased when dealing with small targets. We suggest the max-filter, harmonic mean-filter, and geometric mean filters with protective window to address this issue. One area that is not included in the suggested protective window solution is the area around pixel (i, j). This area, known as the protective window, is cantered on the observed pixel (i, j) and is not affected by the actions of the three filters mentioned above. Its size is (2P+1), X(2P+1). 'P' ought to be smaller than 'N (P < N).'
The protective window is utilized to gather background samples from the immediate area.
We have selected the following window combinations [Table1] with sizes (2N+1) X (2N+1) and for the simulation, the protective window has sizes of (2P + 1) X (2P + 1).

Table 1: Combinations of a protective window (Size (2P+1) X(2P+1)) with a window (size 2N+1) X (2N+1), (P<N).

(2N+1) X (2N+1)	(2P+1) X (2P+1)
N=2	P=1
N=3	P=1,2
N=4	P=1,2,3

In order to conduct a quantitative comparison between the techniques, the filtered image's SNR (Signal to Noise Ratio) is computed using the following relation.

$$SNR_{out} = 20\log_{10}\left(\frac{t_{max} - m'_B}{\sigma_B}\right)$$

Where t_{max} = peak value of the target
$m_{,B}$ = mean variance of the background
σ_B = standard deviation of the background

Simulation Result: A medical image of the brain (MRI of Brain Matlab Image) is taken for modelling purposes. This is even morehazy. The SNR at the noise removal system's output (SNR out) for a certain value of the SNR in the original picture (SNR min) indicates how resilient the system is to target leakage. The selection of SNR in therefore becomes problematic while simulating the targets. Naturally, the algorithm's performance is impacted by the parameter selection. In order to assess the algorithms, we constructed a synthetic target with predetermined SNR in values, such as 2, 4, 6, 8 and 10 dB. We selected low SNR values to approximate the worst-case scenario for background removal techniques impacted by target-induced bias in the background estimation. The picture frame is of size 100 X100.

The algorithms have been put to the test on noisy and blurry images

Each algorithm's performance in relation to the 2-D sliding window's size has been tested by evaluating, SNR out for a range of N values. It is impossible to establish a unique link between SNR out and N. SNR out actually depends on the filter length and the properties of the background area around the target pixel for each technique.
The following four scenarios have been used to evaluate the algorithms for simulation: Max-, Harmonic mean, Geometric mean, Max-P, Harmonic-P, and Geometric mean- P filters.

Graphical result using the geomean, max, and harmonic-mean filters

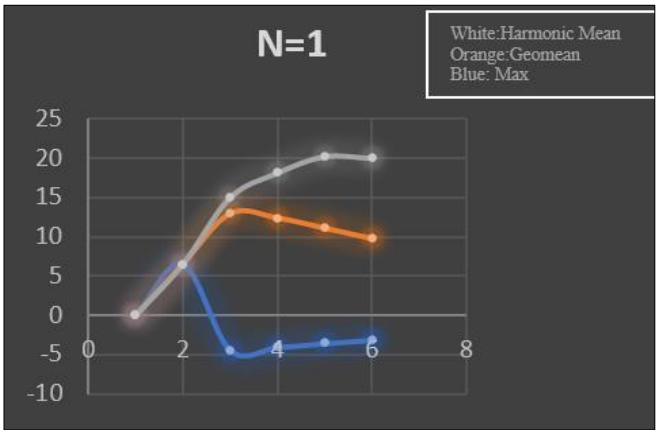

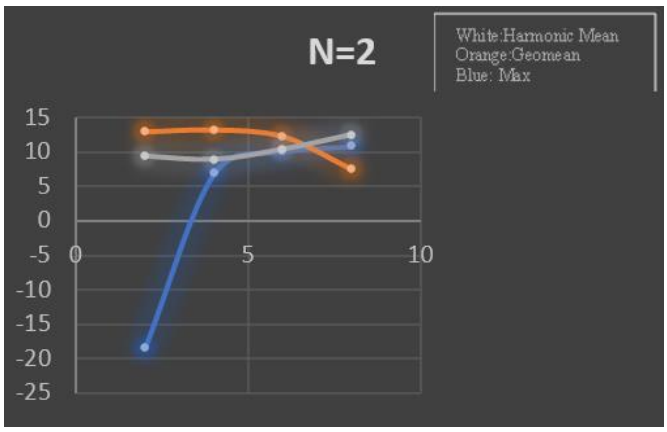

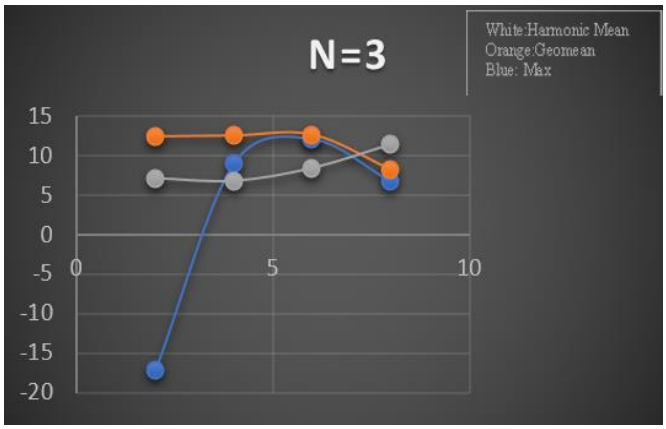

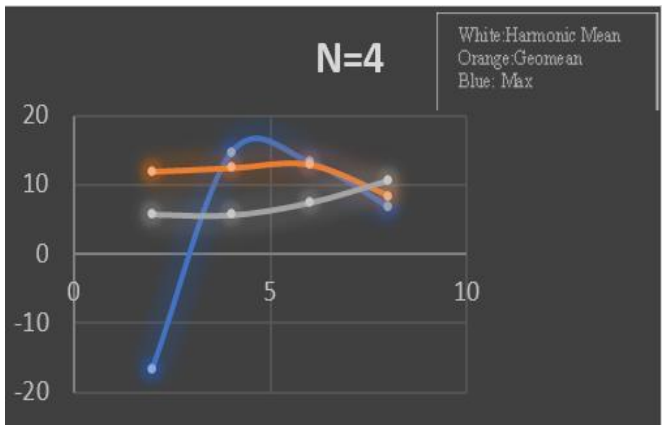

Graphical result by max-filter, harmonic-filter, geomean-filter with protective window

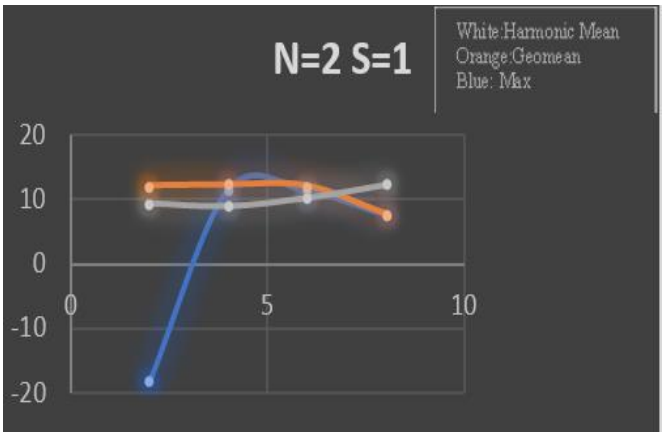

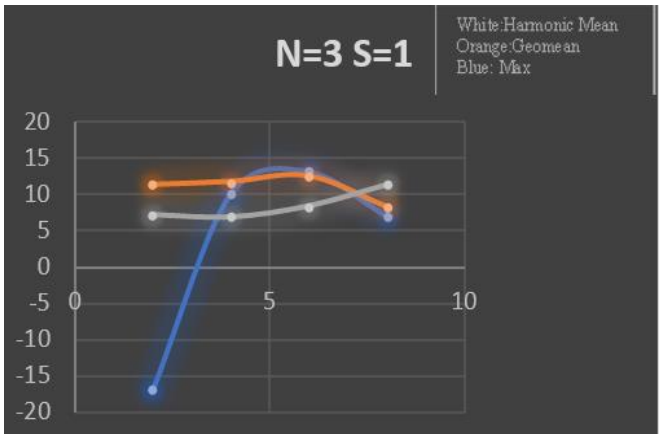

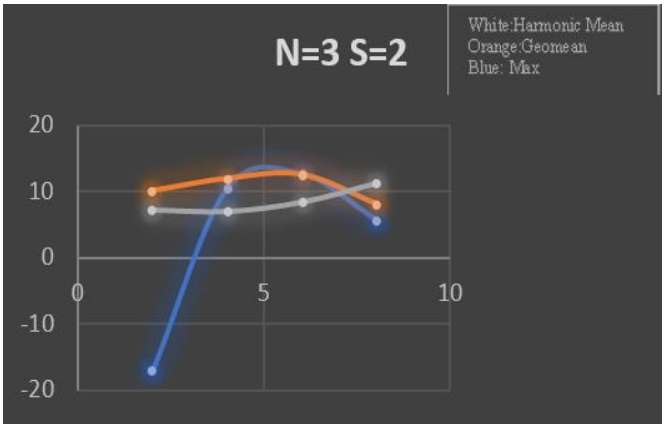

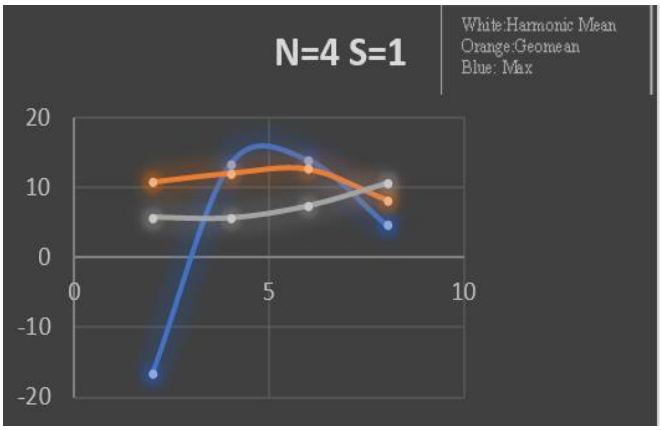

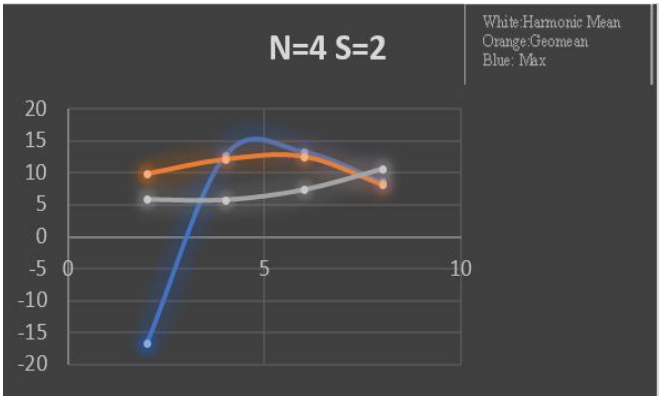

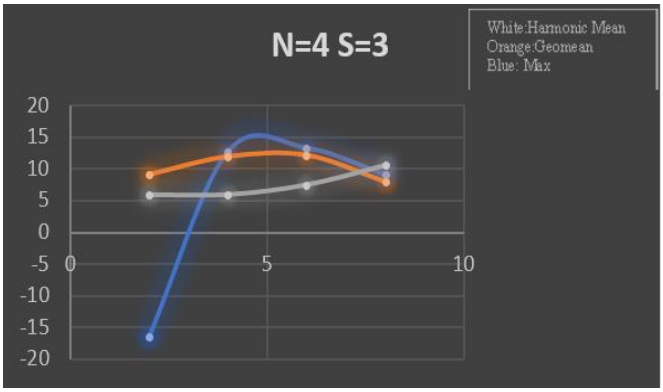

Conclusion

This study compares the efficacy of background removal methods based on three distinct 2-D filters: Geometric mean, max, and harmonic mean filters. To lessen the bias brought on by the target, a modified version of these three algorithms has also been devised, complete with a protective window. By defining SNR out, the capacities to suppress the background structure and preserve the target of interest have been objectively assessed. The outcomes also demonstrate that the Geometric-mean approach, which preserves the target with a very low SNR of about 2dB, is more effective when a protective window is introduced.

References

1. Li C. A partial differential equation-based image restoration method in environmental art design. Adv Math Phys. 2021;2021:1-11. https://doi.org/10.1155/2021/4040497.
2. George A, Rajakumar B, Suresh B. Markov random field-based image restoration with aid of local and global features. Int J Comput Appl. 2012;48(8):23-28. https://doi.org/10.5120/7369-0137.
3. Wagadre K, Singh M. Wavelet transform based fusion technique for image restoration. Int J Comput Appl. 2016;153(12):18-20. https://doi.org/10.5120/ijca2016912208.
4. Maru M, Parikh M. Image restoration techniques: A survey. Int J Comput Appl. 2017;160(6):15-19. https://doi.org/10.5120/ijca2017913060.
5. Gupta S, Porwal R. Implementing blind de-convolution with weights on x-ray images for lesser ringing effect. Int J Image Graphics Signal Process. 2016;8(8):30-36. https://doi.org/10.5815/ijigsp.2016.08.05.
6. Taherinia A, Fotouhi M, Jamzad M. A new watermarking attack using long-range correlation image restoration. https://doi.org/10.1109/ares.2009.131.
7. Sharma T. Various types of image noise and de-noising algorithm. Int J Mod Educ Comput Sci. 2017;9(5):50-58. https://doi.org/10.5815/ijmecs.2017.05.07.
8. Jiang B, Yang A, Wang C, Hou Z. Comparison of motion-blurred image restoration using wiener filter and spatial difference technique. Int J Signal Process Image Process Pattern Recognit. 2014;7(2):11-22. https://doi.org/10.14257/ijsip.2014.7.2.02.
9. Jain AK. Fundamentals of Digital Image Processing. Pearson Prentice Hall; c2015.
10. Han Y. Enhanced mask R-CNN blur instance segmentation based on generated adversarial network. https://doi.org/10.1117/12.2685510.
11. Du Z. Unsupervised neural network-based image restoration framework for pattern fidelity improvement and robust metrology. J Micro/Nano patterning Mater Metrology. 2023;22(03). https://doi.org/10.1117/1.jmm.22.3.034201.
12. Ayu M, Permana I. The discrete wavelet transforms based iris recognition for eyes with non-cosmetic contact lens. Iaes Int J Artif Intell (Ij-Ai). 2023;12(3):1118. https://doi.org/10.11591/ijai.v12.i3.pp1118-1127.
13. Li K. A method for restoring γ-radiation scene images based on spatial axial gradient discrimination. Electronics. 2023;12(17):3734. https://doi.org/10.3390/electronics12173734.
14. Wang K. On-earth observation of low earth orbit targets through phase disturbances by atmospheric turbulence. Remote Sensing. 2023;15(19):4718. https://doi.org/10.3390/rs15194718.
15. Dong J. Multi-scale residual low-pass filter network for image deblurring. https://doi.org/10.1109/iccv51070.2023.01134.
16. Prajapati R. Design of hybrid adaptive model for image denoising. International J Sci Res Eng Manag. 2023;07(11):1-11. https://doi.org/10.55041/ijsrem27371.
17. Li Y. Wig-net: Wavelet-based defocus deblurring with ifa and GCN. Appl Sci. 2023;13(22):12513. https://doi.org/10.3390/app132212513.
18. Kiyokawa T, Takamatsu J, Koyanaka S. Challenges for future robotic sorters of mixed industrial waste: A survey. IEEE Trans Autom Sci Eng. 2024;21(1):1023-1040. https://doi.org/10.1109/tase.2022.3221969.